

1 **Pan-neuronal expression of human mutant Huntingtin protein in *Drosophila* impairs**
2 **immune response of hemocytes**

3 Jyoti Dhankhar^a, Namita Agrawal^{a*}, Anju Shrivastava^{a*}

4 Authors' affiliations-

5 **a** Department of Zoology, University of Delhi, Delhi-110007, India

6

7 *** Corresponding authors-**

8 **Prof. Anju Shrivastava**

9 Department of Zoology

10 University of Delhi

11 New Delhi-110007, India

12 E mail: anjushrivastava.du@gmail.com; ashrivastava@zoology.du.ac.in

13 Voice: +91-9811900814

14 **Prof. Namita Agrawal**

15 Department of Zoology

16 University of Delhi

17 New Delhi-110007, India

18 E mail: nagrawaluci@gmail.com; nagarwal@zoology.du.ac.in

19 Voice: +91-9717412612

20 **Contributing author-**

21 **Jyoti Dhankhar-** jyotidhankhar37@gmail.com

22 **Acknowledgement:** All authors are in agreement with the content of the manuscript.

23

24 **Abstract**

25 Huntington's disease (HD) is a late-onset; progressive, dominantly inherited neurological
26 disorder marked by an abnormal expansion of polyglutamine (poly Q) repeats in Huntingtin
27 (HTT) protein. The pathological effects of mutant Huntingtin (mHTT) are not restricted to
28 the nervous system but systemic abnormalities including immune dysregulation have been
29 evidenced in clinical and experimental settings of HD. Indeed, mutant huntingtin (mHTT) is
30 ubiquitously expressed and could induce cellular toxicity by directly acting on immune cells.
31 However, it is still unclear if selective expression of mHTT exon1 in neurons could induce
32 immune responses and hemocyte function. In the present study, we intended to monitor
33 perturbations in the hemocytes population and their physiological functions in *Drosophila*,
34 caused by pan-neuronal expression of mHTT protein. We found that pan-neuronal expression
35 of mHtt significantly alters crystal cells and plasmatocyte count in larvae and adults with
36 disease progression. Interestingly, plasmatocytes isolated from diseased conditions exhibit a
37 gradual decline in phagocytic activity *ex vivo* at progressive stages of the disease as compared
38 to age-matched control groups. We also observed an increased production of reactive oxygen
39 species (ROS) in plasmatocytes at advanced stages of the disease. In addition, diseased flies
40 displayed elevated reactive oxygen species (ROS) in circulating plasmatocytes at the larval
41 stage and in sessile plasmatocytes of hematopoietic pockets at of disease. All the parameters
42 were monitored progressively, targeting the circulation at larvae stage and hematopoietic
43 pockets in adults at different disease stages, and many alterations were documented in the
44 early stage itself. These findings strongly implicate that neuronal expression of mHtt alone is
45 sufficient to induce non-cell-autonomous immune dysregulation *in vivo*. Based on these
46 findings, we propose that further insight into the mechanisms through which neuronal
47 expression of mHtt might be inflicting the innate immune responses would facilitate
48 therapeutic inventions aimed at amelioration of HD pathology and improving the quality of
49 life of the patients.

50 **Key words:** Huntington's disease, transgenic *Drosophila*, immune response, phenoloxidase
51 activity, phagocytosis, reactive oxygen species

52 **1. Introduction**

53 Huntington's disease (HD) is a rare, dominantly inherited progressive neurodegenerative
54 disorder caused by an unstable expansion in the polymorphic CAG trinucleotide repeat in
55 exon 1 of Interesting Fragment 15 (IT15) gene on chromosome 4, which is ubiquitously
56 expressed (Hoogeveen et al., 1993; MacDonald et al., 1993; Marques Sousa & Humbert,
57 2013). Mutant Huntingtin (mHTT) protein harbors an expanded polyglutamine tract beyond
58 35 repeats that confer toxic gain of function and causes severe neuronal degeneration in the
59 striatum and cortical regions of brain; that results in motor impersistence, cognitive decline,
60 psychiatric abnormalities leading to gradual loss of functional capacity and eventually death
61 (Bates et al., 2002; Ho et al., 2001). This devastating disease has late-onset typically at 40s
62 and 50 years of life and is inversely related to the number of CAG repeats (Andrew et al.,
63 1993). The traditional research in HD focuses on preferential neuronal dysfunction in the
64 specific brain regions resulting in characteristic clinical symptoms; however, emerging
65 evidence indicates that mHTT might affect the region beyond the central nervous system
66 (CNS). Besides neuronal deposition of mHTT, other mechanisms such as oxidative stress,
67 free radicals, dysregulated immune response including inflammation seem to contribute to
68 HD pathogenesis and progression (Kotrcova et al., 2015; Tai et al., 2007). Abnormal
69 phenotypic effects caused by the expression of mHTT in various non-neuronal, peripheral
70 cells and tissues have been described in skeletal muscles, cardiac muscles, adipose tissues,
71 fibroblasts, and immune cells of HD animal models and patients (Björkqvist et al., 2008;
72 Moffitt et al., 2009; Sassone et al., 2009; Sathasivam et al., 1999).
73 Abnormalities related to immune system in particular, have been reported in several animal
74 HD models and HD patients (Andre et al., 2016; Leblhuber et al., 1998). Expression of

75 mHTT in astrocytes of transgenic R6/2 mice model induces age-dependent neurological
76 phenotypes such as weight loss, motor deficits, and early death (Bradford et al., 2009). In
77 healthy state, microglia the key player of cerebral innate immune system remains quiescent
78 and regulates immune response by producing anti-inflammatory and neurotrophic factors
79 (Streit., 2002). Activation of microglia can induce neuronal damage via several mechanisms
80 such as production of free radicals, caspase activation, and excitotoxicity (Crotti et al., 2014;
81 Hanisch, 2002; Kim & de Vellis, 2005; Wang et al., 2004). In this regard, a set of studies
82 have shown that increased expression of cannabinoid receptor 2 (CB2) attenuates activation
83 of microglia and peripheral immune cells and thus suppresses disease pathogenesis in HD
84 mice model (Bouchard et al., 2012; Palazuelos et al., 2008). The expression of mutant protein
85 induces activation of both brain and peripheral immune cells in HD patients and in mouse
86 models. In a report, upregulation of pro-inflammatory cytokines such as IL-6, IL-12, tumor
87 necrosis factor (TNF α), and acute-phase protein α 2-microglobulin clusterin (involved in
88 clearance of cellular debris in cerebrospinal fluid (CSF) and plasma of HD patients was
89 observed (Björkqvist et al., 2008). A recent study also showed increased levels of pro-
90 inflammatory and regulatory cytokines such as IL-4, IL-6 IL-12, and TNF α in vital peripheral
91 organs i.e. liver, heart, spleen, and kidney of BACHD mice model (Valadão et al., 2019).
92 Besides, microglia and peripheral immune cells, human HD patients exhibited impaired
93 migration and recruitment of chemotactic stimuli (Kwan et al., 2012). Taken together, these
94 reports suggest that innate immune dysfunction plays an important role in HD pathogenesis.
95 However, the interaction between CNS pathology and changes in peripheral immune cells in
96 HD patients is poorly understood but can be of utmost importance in suppressing disease
97 progression. Additionally, few recent studies reported that ectopic expression of mHTT
98 expression in immune cells leads to altered immune responses, higher susceptibility against

99 infectious agents, and premature mortality in animal HD models (Donley et al., 2016; Lin et
100 al., 2019).

101 *Drosophila melanogaster* is a well-established animal model for HD studies.
102 Despite apparent differences between humans and flies, several biological mechanisms are
103 highly conserved across evolution such as networking of complex nervous system, genetic
104 mutations, innate immunity control, and biological rhythms (Jennings, 2011; Lemaitre &
105 Hoffmann, 2007; Zehring et al., 1984). Moreover, key aspects of *Drosophila* immunity
106 possess striking similarities with mammalian innate immunity (Dhankhar et al., 2020). Innate
107 immunity of fruit fly constitutes humoral and cellular defense mechanisms. Humoral
108 immunity involves the production of antimicrobial peptides (AMPs) from the fat body;
109 however, cellular immunity is mediated by three types of hemocytes: plasmatocytes, crystal
110 cells, and lamellocytes. Plasmatocytes are responsible for phagocytosing invading pathogens
111 and apoptotic debris and represent the functional equivalent of mammalian macrophages
112 (Elrod-Erickson et al., 2000). Crystal cells contain crystalline inclusions of phenoloxidase
113 enzyme which is released during melanization, a process required for successful wound
114 healing. Lamellocytes are the cryptic, stress-induced cell type that is responsible for
115 encapsulation of objects that are too large to be phagocytosed such as eggs of parasitic wasps
116 (Meister & Lagueux, 2003). These hemocytes reside in three major compartments: in the
117 circulation, lymph gland, and the hematopoietic pockets segmentally distributed on both sides
118 of dorsal vessel.

119 The expression of human *mHTT* exon 1 fragment with expanded CAG repeats in the
120 neuronal tissue of transgenic flies causes neurodegeneration *in vivo* and recapitulate the
121 characteristic feature of HD including gradual accumulation of mHTT aggregates in neural
122 cells and subsequent apoptosis, transcriptional dysregulation, motor abnormalities, and
123 ultimately death similar to those in human patients (Steffan et al., 2001; Taylor et al., 2003).

124 Furthermore, *Drosophila* provides an excellent system for spatiotemporal expression of
125 transgenes using the bipartite UAS-GAL4 system and evaluating direct effects of transgene in
126 an *in vivo* condition (Brand & Perrimon, 1993; Marsh et al., 2000). The present study aimed
127 to elucidate major changes occurring in the hemocyte population and their physiological
128 functions in the *Drosophila* model of HD when exon 1 fragment of human mHTT selectively
129 expressed in neuronal cells. To experiment, UAS-GAL4 system was used to express mHTT
130 with pan-neuronal elav-Gal4 driver and investigated possible repercussions of neuronal
131 mHTT on hemocytes of transgenic *Drosophila*. Interestingly we found that the expression of
132 mHTT in neural cells affects hemocyte population and alters their functional abilities which
133 include melanization, phagocytosis of infectious agent, and production of reactive oxygen
134 species. Altogether, our findings suggest that amendment in innate immune response in HD
135 flies might be due to an indirect effect of mHTT on the integrated process of immune
136 regulation, which may occur due to extensive neuronal impairment mimicking disease
137 condition. Therefore, identification of new therapeutic targets aimed towards immune
138 regulation may be effective in delaying disease progression and improving the quality of life
139 of the patient's.

140 **2. Materials and Methods**

141 **2.1. *Drosophila* stocks and crosses.** *Drosophila* cultures were grown at 25°C and 65%
142 humidity on standard cornmeal under a constant 12h light: 12h dark cycle. Expression of
143 transgene human HTT exon1 fragment containing polyglutamine repeats carried out using the
144 bipartite UAS-GAL4 expression system. Transgenic stocks used in this study include *w*;
145 P{*w+mW.hs=GawB*}*elavC155*: a pan-neuronal driver (#8765; BDSC), *w*; P{UAS-*Httex1p*
146 Q25}, and *w*; P{UAS-*Httex1p* Q93}4F1 ; generously gifted by Prof. J. Lawrence Marsh,
147 UCI, Irvine, California. Virgin females from UAS-*Httex1p* Q25 (wild type) and UAS-
148 *Httex1p*Q93 (mutant) were mated with the males of *elav-GAL4* and resulting female

149 progenies elav>Httex1p Q25 (controls) and elav>Httex1p Q93 (diseased) were used for all
150 the assays. All animal experiments were conducted following the national and international
151 guidelines and the relevant national laws on the protection of animals. All experiments of this
152 study were conducted using *Drosophila* and it remains out of bioethical considerations.

153 **2.2. Crystal cell melanization assay.** For crystal cell visualization, at least 10 wandering 3rd
154 instar larvae of both control and diseased conditions were kept in 1ml of 1X PBS in glass
155 vials and incubated at 65°C for 10 mins. Heat-shocked larvae from each condition were then
156 arranged on a glass slide over a black background and imaged using Nikon SMZ 745T
157 stereozoom microscope right after heating. Melanized crystal cells appeared as black puncta
158 on larval cuticle in three posterior-most abdominal segments A6, A7 and A8 were quantified
159 using ImageJ software. Minimum three replicates (10 larvae/replicate) per condition were
160 used for the assay.

161 **2.3. Estimation of phenoloxidase activity.** For estimation of phenoloxidase (PO) activity, 10
162 individuals of each condition were homogenized in homogenization buffer (containing
163 protease inhibitor (Sigma-Aldrich, S8820) and then centrifuged at 13000 rpm for 10 mins.
164 The supernatant was collected in fresh pre-chilled eppendorf and the protein concentration of
165 each sample was estimated using Bradford assay (Bradford, 1976). PO activity in the
166 supernatant was quantified using a microplate enzyme assay. A reaction mixture having
167 protein concentration of 10µg/µl was prepared by diluting the supernatant in 1X PBS
168 containing protease inhibitors. 50 µl of each sample was then plated in 96 well plate and
169 added 50 µl of 3mM L-3-4-dihydroxyphenylalanine (L-DOPA) (substrate for enzyme
170 phenoloxidase) to each well and incubated at 25°C for 30 min. Absorbance was measured at
171 492nm using an ELISA plate reader (Biotek). Minimum three replicates per condition were
172 used for the assay.

173 **2.4. Plasmacytes Isolation**

174 a) **Isolation of circulating plasmatocytes from larvae:** Wandering 3rd instar larvae
175 were collected from the wall of food vials in a petri-plate having wet filter paper to
176 remove the food debris present on the larval cuticle. The larvae were then placed on
177 ice to slow down their movement. Seven larvae of each condition were placed in
178 100µL of 1X PBS in a cavity block. Using a pair of fine tweezers, the cuticle of the
179 larvae was pinched very slightly to release the hemolymph into the media while
180 avoiding gut breaking. Hemolymph samples were collected and placed on ice for
181 further analysis. Analysis was performed just after the dissection to avoid
182 melanization reactions in the hemolymph.

183 b) **Isolation of plasmatocytes from hematopoietic pockets of adult flies:** Anesthetized
184 flies were positioned dorsal side down in a drop of PBS on a clean glass slide. Using
185 the needles, the wings stretched apart to ensure that the dorsal abdomen submerged in
186 1X PBS. A fine incision is then made from the posterior tip of the fly abdomen
187 ventrally and continued up to the head. The dissected fly body part consists of the
188 dorsal side of the thorax and abdomen. The tissues present inside the abdominal
189 cavity like gut, ovaries, Malpighian tubules were gently removed while the dorsal
190 abdominal diaphragm is kept untouched. Ten dissected abdomen cuticles were placed
191 in 100µl of 1X PBS in a cavity block and disturbed with the help of a needle to
192 release hemocytes from the pockets. The resulting hemocytes suspension was
193 collected in pre-chilled eppendorf for further analysis

194 **2.5. Screening of plasmatocytes.** Isolated hemolymph/ plasmatocytes suspension was plated
195 on the pre-cleaned slides and placed in a humidified chamber for adherence of plasmatocytes
196 for an hour at 25°C. After incubation, slides were washed with 1X PBS to remove non-
197 adherent cells. Adhered plasmatocytes were fixed in 100% methanol for 30 seconds; air-dried
198 and stained with 0.2% crystal violet (HiMedia, RM114) stain for 90 seconds. Preparations

199 were mounted in DPX and images were taken at different magnifications under the Nikon
200 Eclipse E-100 microscope.

201 **2.6. Plasmatocytes counting.** To evaluate plasmatocyte count, we prepared a 1:1 dilution of
202 hemolymph/plasmatocytes suspension with the 0.4% trypan blue solution (Himedia, TC193)
203 and pipetted several times to ensure a uniform cell suspension. 10 μ L of trypan blue-cell
204 suspension was loaded on a hemocytometer carefully by touching the coverslip at its edge
205 with the pipette tip. Hemocytometer was then observed under the Nikon microscope at 10x
206 magnification and cells were counted in four outer squares in the grid (each square contains
207 16 smaller squares). The average plasmatocyte count per individual was then calculated using
208 the given formula.

$$209 \text{ Average cell count per larva/fly} = \frac{\text{Average cell count per square} \times \text{Total volume of sample} \times \text{D.F.}}{\text{No. of larvae per sample}}$$

211 **2.7. Staining of bacteria.** Overnight grown *E. coli* culture was harvested by centrifugation at
212 10,000 rpm for 10 minutes and washed three times with 1X PBS to remove LB.
213 Subsequently, bacteria were heat-killed at 90°C for an hour. Heat killed bacteria again
214 washed three times with 1X PBS and incubated with 10 μ g/ml propidium iodide (PI) (Sigma-
215 Aldrich, P4170) stain for an hour on a shaker at room temperature. Finally, bacteria were
216 washed with 1X PBS and diluted to a concentration of 10⁸ bacterial cells/ml. Bacterial
217 concentration was checked by measuring optical density at 600 nm (OD₆₀₀) (modified from
218 Neyen et al., 2014).

219 **2.8. Phagocytic assay.** To assess phagocytosis, 100 μ L volume of cell suspension ($\sim 3 \times 10^4$
220 cells) was plated on pre-cleaned slides and incubated in a humidified chamber at 25°C for an
221 hour for adherence of plasmatocytes. The number of larvae/adults to sacrifice depends on the
222 genotype. After incubation, slides were washed with 1X PBS to remove non-adherent cells.
223 After that heat-killed PI-stained *E. coli* (100 μ l of 10⁸ cells/ml of suspension) was added to the

224 slide and again incubated for 40 mins at 25°C to enable phagocytosis. Slides were then
225 washed to remove un-phagocytosed bacteria, methanol fixed and air-dried and mounted with
226 Vectashield media containing DAPI (Vector laboratories, H1200). The slides were observed
227 under confocal microscope and percent phagocytosis was calculated by counting the number
228 of plasmacytes showing phagocytosis per 100 plasmacytes. Minimum five replicates per
229 condition were used for the assay.

230 **2.9. Estimation of nitric oxide production.** The production of nitric oxide (NO) was
231 estimated from the accumulation of nitrite, a stable end product of nitric oxide, by the
232 activated plasmacytes using Griess reagent (Ding et al., 1988). Briefly, 1×10^5 cells of each
233 genotype were plated in 96 well plate and left for an hour at 25°C for adherence. The adhered
234 cells were then treated with LPS (10µg/ml) and heat-killed *E. coli* (100µl of 10^8 cells/ml of
235 suspension) and further incubated at 25°C. After 48 hrs of treatment, 25µL of culture soup
236 from each well was taken and centrifuged at 12000 rpm for 5 mins to remove cells from the
237 soup. 20µL of supernatant was taken, added an equal volume of freshly prepared Griess
238 reagent (1:1 of 1% sulphanilamide in 2.5% H₃PO₄ and 0.1% ND in distilled water) and
239 incubated at room temperature for 10 mins. Absorbance was measured at 540 nm on an
240 ELISA plate reader (Biotek). Nitrite concentrations were estimated by extrapolation from the
241 sodium nitrite standard curve. Minimum three replicates per condition were used for the
242 assay.

243 **2.10. Reactive oxygen species (ROS) estimation.** Dihydroethidium (DHE) staining was
244 used to monitor superoxide radicals in the plasmacyte isolated from healthy and diseased
245 conditions. 1×10^4 plasmacytes of each condition were plated on the pre-cleaned coverslips
246 and left for adherence for an hour at 25°C. Cells were washed with 1X PBS to remove excess
247 of bacteria. A stock solution of 30mM DHE (Invitrogen Molecular Probes, D11347) was
248 reconstituted in anhydrous dimethyl sulfoxide (DMSO, Sigma-Aldrich, 276855). For

249 staining, the reconstituted dye was further diluted in 1X PBS to obtain a final working
250 concentration of 25 μ M. The cells were incubated with dye for 10 mins in dark. This was
251 followed by rinsing of cells with 1X PBS and mounting with Vectashield media containing
252 DAPI. Images were acquired immediately under the Nikon Eclipse (Ni-E) fluorescence
253 microscope and fluorescence intensity quantification was performed using ImageJ software.
254 Minimum five samples per condition were analyzed for ROS quantification.

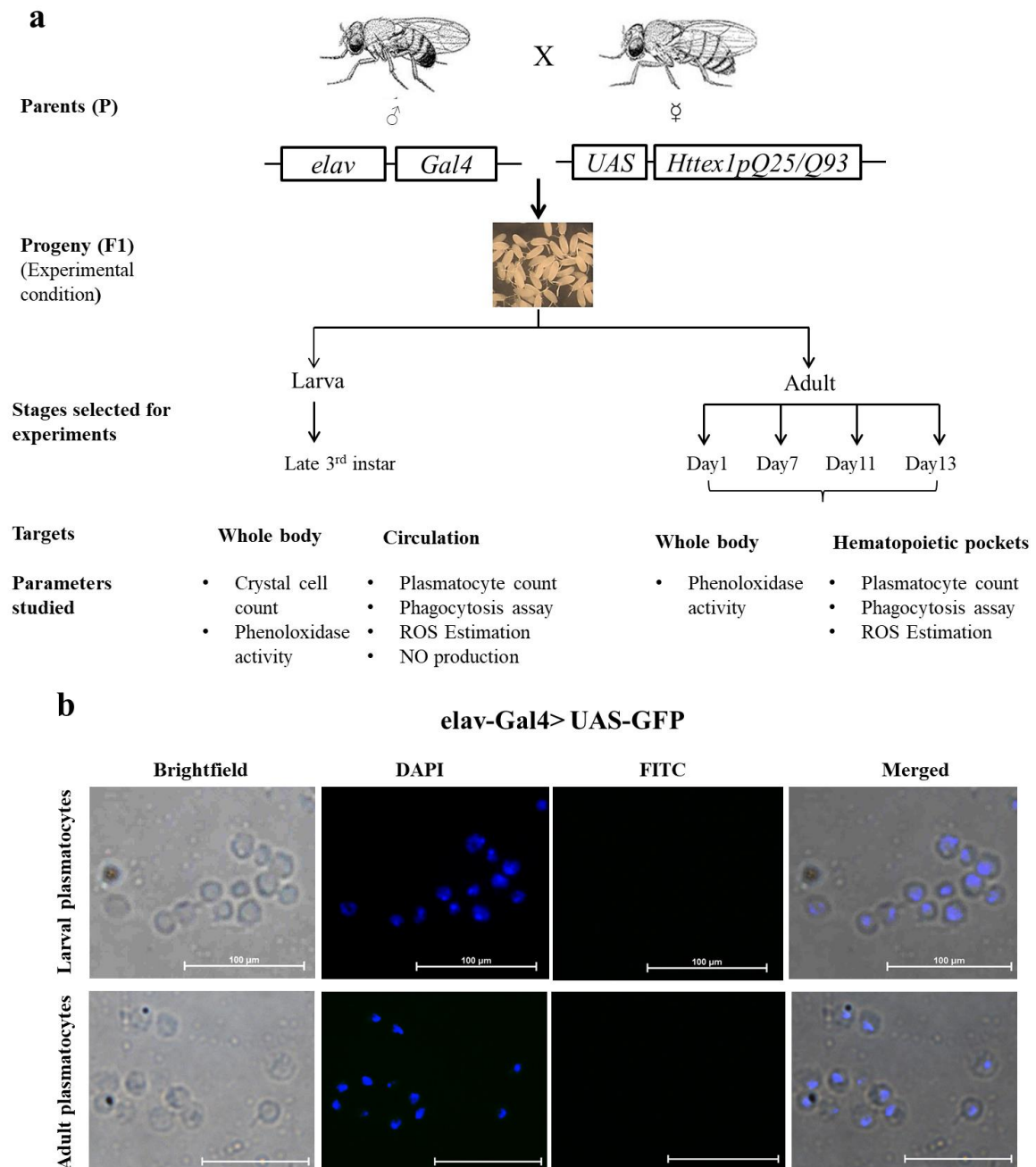
255 **2.11. Statistical analysis.** All the graphically presented values represent the mean value.
256 Normality of data sets was determined using the Shapiro-Wilk test. Data analysis of normally
257 distributed data was done by Student's t-test for pair-wise comparison. All statistical analysis
258 was performed using the IBM SPSS package. P-value 0.05 was considered statistically
259 significant. The p-value ≤ 0.05 marked as *, p-value ≤ 0.01 marked as **, p-value ≤ 0.001
260 marked as ***. All experiments were repeated 3-4 times as per requirement.

261 **3. Results**

262 **3.1. Experimental scheme**

263 In present study, expression of transgene human HTT exon1 fragment containing unexpanded
264 and expanded polyglutamine repeats was carried out using the bipartite UAS-GAL4
265 expression system so that subsequent progeny mimic the disease symptoms. All the
266 experiments were performed at two developmental stages of *Drosophila* i.e. late 3rd instar
267 larvae indicating the early manifestation stage of disease and adult flies at indicated ages
268 representing the disease's progressive stages. We targeted the circulating system at the larval
269 stage and hematopoietic pockets in adults for quantification of plasmatocytes and their
270 functional activities. However, crystal cell count and phenoloxidase activity was appraised in
271 the whole body of larvae and adults. In addition, to ensure that elav-Gal4 driver is exclusively
272 expressed in pan neurons but not in immune cells, we examined elav-GAL4 (elav-
273 GAL4>UAS-GFP) expression by GFP reporter throughout different developmental stages.

274 By microscopic observation, it was evident that *elav* is neither expressed in plasmatocytes at
 275 larval and adult stage (fig.1b). Hence, it can be concluded that immune cells are completely
 276 devoid of *elav*-Gal4 expression.



277 **Figure 1. Outline of experimental scheme and visualization of *elav* driven GFP**
 278 **expression in plasmatocytes of larvae and adult flies. (a) Schematic representation of**
 279 **research design and parameters studied, (b) Microscopic visualization of plasmatocytes**
 280

281 isolated from 3rd instar larvae and adults confirmed lack elav driven GFP expression in
282 immune cells.

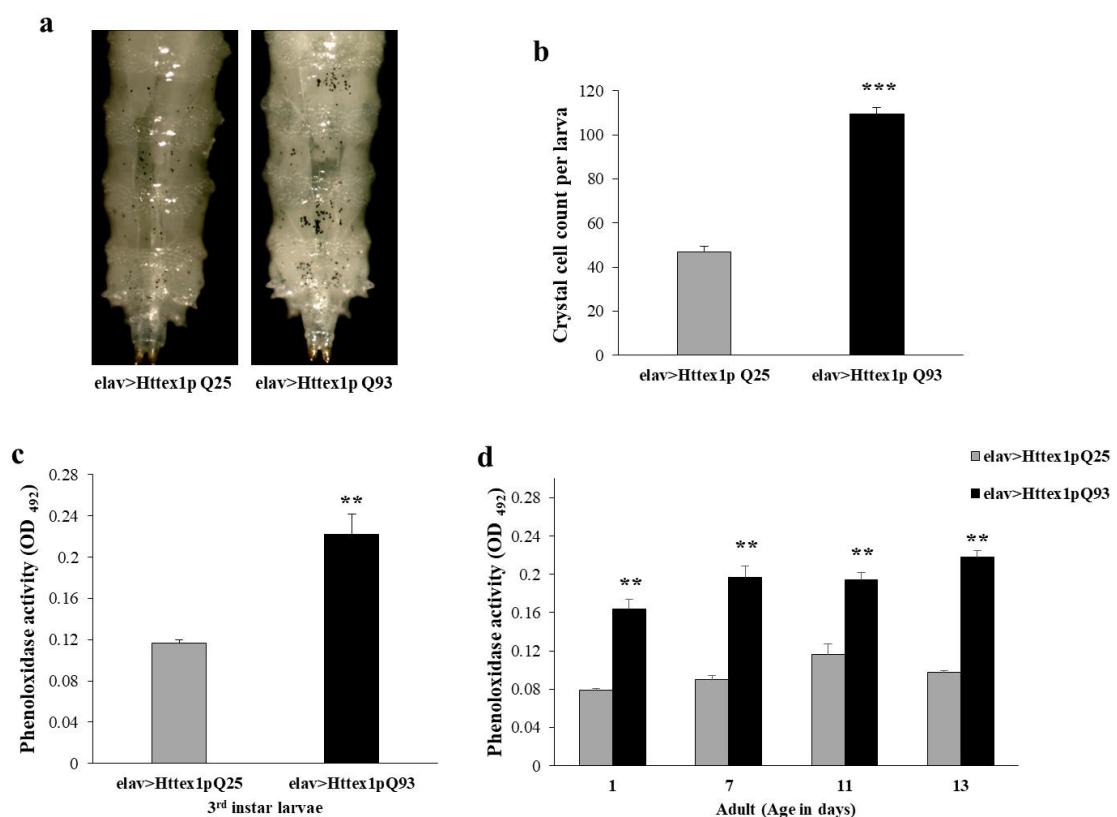
283 **3.2. Neuronal expression of Httex1p Q93 causes alteration in crystal cell count and** 284 **phenoloxidase activity in HD condition.**

285 Abnormalities related to the immune system were observed in several studies of HD patients. In an attempt to delineate the immune response
286 anomalies associated with HD, we used transgenic flies expressing human HTT exon1 with
287 unexpanded polyQ tract (Httex1p Q25, wild type) and expanded polyQ tract (Httex1p Q93,
288 mutant) under the control of elav-GAL4 driver since the embryonic stage.

289 Crystal cells serve as a critical indicator of *Drosophila's* stress status and any abnormal
290 change in crystal cell count and their activity can be the first crucial sign for outlining the
291 alteration in immune response. To better understand the involvement of immune system in
292 Huntington's disease and its progression, we primarily sought to discern the alterations, if
293 any, in crystal cell number in elav>Httex1p Q25 (control, referred hereafter 25QHtt^{ex1}) and
294 elav>Httex1p Q93 (diseased, referred hereafter 93QHtt^{ex1}) larvae. Heat shock to larvae in
295 PBS at 67°C causes spontaneous activation of the prophenoloxidase zymogen within crystal
296 cells, leading to their blackening, and consequently making them visible through the cuticle
297 as black puncta (Rizki et al., 1980). Surprisingly, a higher number of black puncta were seen
298 in three posterior abdominal segments (A6, A7, and A8) of diseased larvae (Fig.2a).
299 Numerical variation in crystal cell count was quantified using ImageJ software.
300 Quantification result confirmed that 93QHtt^{ex1} larvae show significant increase in crystal cell
301 number (n = 10, p = 5.66397E-12) (Fig. 2b) than age-matched controls. This prominent
302 change in crystal cell population could be a reflection of amended/altered immune response
303 in HD pathogenesis.

304 As more melanization dots were observed on the cuticle of diseased larvae, we further
305 measured enzymatic phenoloxidase (PO) activity with an L-DOPA assay in the hemolymph

306 of larvae and adults with disease progression. Phenoloxidase is a key enzyme in the
 307 melanization process that catalyzes the oxidation of phenols to quinones, which subsequently
 308 polymerize into melanin. Diseased larvae showed significantly higher PO activity ($n = 3$; $p =$
 309 0.009782) (Fig. 2c) as compared to age-matched controls. Similarly, diseased flies had
 310 significantly higher PO activity at the indicated ages compared to controls ($n = 3$; day 1, $p =$
 311 0.009782 ; day 7, $p = 0.006137$; day 11, $p = 0.006178$; day 13, $p = 0.002072$) (Fig. 2d). These
 312 results together support that crystal cell population and function remain altered in HD flies.



313 **Figure 2. Increased crystal cell count and phenoloxidase activity in diseased condition.**
 314

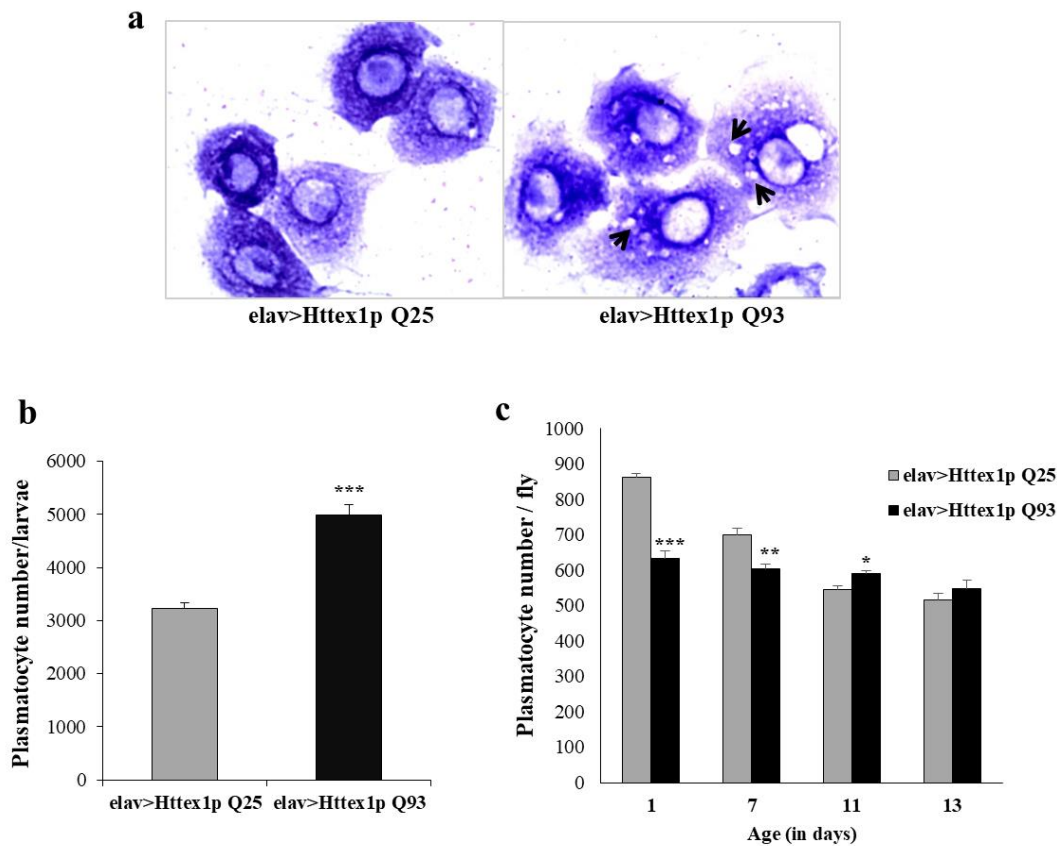
315 (a) Crystal cells in the posterior abdominal segments of 93QHtt^{ex1} (diseased, right panel) and
 316 25QHtt^{ex1} expressing (control, left panel) 3rd instar larvae. (b) Circumferential crystal cells
 317 were counted from the three posterior segments A6, A7, and A8 of the heat-shocked control
 318 and diseased third instar larvae. Diseased larvae (black bar) displayed a significant increase in
 319 crystal cell number as compared to age-matched control (grey bar). Crystal cells were

320 quantified using imageJ software. Error bars represent \pm SEM (n=10/genotype); P-value:
321 *** $P < 0.001$. Diseased larvae (black bar) (c) and (d) flies exhibit increased phenoloxidase
322 (PO) activity with disease progression as compared to age-matched controls (grey bar). Error
323 bars represent \pm SEM (n=3); P-value: *** $P < 0.001$; ** $P < 0.01$; * $P < 0.05$.

324 3.3. Httex1pQ93 expression causes alteration in plasmatocyte number with disease

325 **progression.** To further extend our observation to decipher the relationship between impaired
326 immune response and Huntington's disease, we evaluated major changes occurring in the
327 plasmatocyte population, major circulating hemocytes of *Drosophila*, and their functional
328 activities induced by neuronal expression of mHTT in larvae and adults at indicated ages. For
329 morphological observations, plasmatocytes adhered to glass slides were stained with 0.2%
330 crystal violet and imaged the Nikon Eclipse E-100 microscope. We observed that
331 plasmatocytes isolated from diseased larvae display heightened cell spreading with extended
332 lamellipodial protrusions and form large vacuoles in the cytoplasm, whereas plasmatocytes
333 isolated from control larvae appeared smaller and round on glass surface (Fig. 3a). The
334 morphological changes of plasmatocytes in larvae prompted us to count their numbers in
335 diseased condition with disease progression. Interestingly, we found that diseased larvae
336 displayed significantly higher number of circulating plasmatocytes (n = 10; $p = 1.89865E-06$)
337 as compared to age-matched control larvae (Fig. 3b). Moreover, an obstinate plasmatocyte
338 count was observed in hematopoietic pockets of diseased flies throughout disease progression
339 from day 1 post eclosion (dpe) to 13dpe, while there was a gradual decline in plasmatocyte
340 number of hematopoietic pockets of controls with aging. During early stage (1dpe and 7dpe),
341 diseased flies had significant lesser number of sessile plasmatocytes (n = 10; 1dpe, $p =$
342 $6.14571E-06$; 7dpe, $p = 0.002965139$) compared to control condition. However, at the
343 advanced ages (11dpe and 13dpe), plasmatocyte count remains persistent in diseased flies
344 and becomes comparable to age-matched controls that showed a significant decline in

345 plasmatocyte count with aging (Fig. 3c). These results indicate that the expression of mHTT
 346 under control of pan-neuronal elav-GAL4 driver alters plasmatocyte population and their
 347 morphological characteristics.

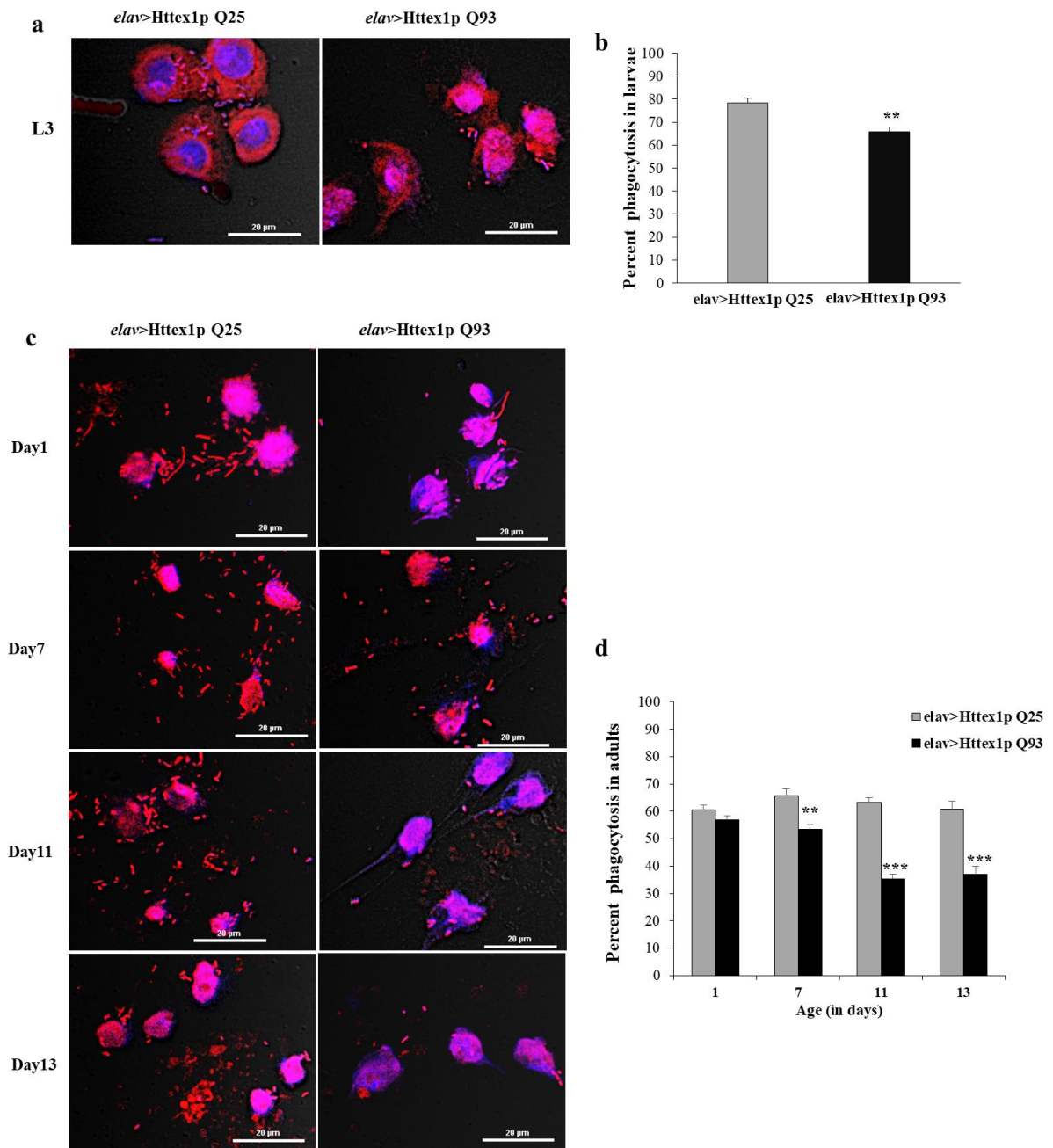


348 **Figure 3. Alteration of plasmatocyte morphology and number in HD condition with**
 349 **disease progression (a)** Images showing characteristic morphology of plasmatocytes isolated
 350 from 25Q Htt^{ex1} (control; left panel) and 93Q Htt^{ex1} expressing larvae (diseased; right panel).
 351 Plasmatocytes isolated from diseased larvae appear more flattened and more dispersed as
 352 compared to the plasmatocytes isolated from control larvae. **(b)** Quantification of
 353 plasmatocytes from the diseased larvae (black bar) showed a significant increase in
 354 circulating plasmatocyte number as compared to age-matched controls (grey bars). **(c)**
 355 Diseased flies exhibit obstinate plasmatocyte count in hematopoietic pockets with disease
 356 progression. Interestingly on day 1 and day 7 diseased flies (black bars) have significant
 357

358 lesser number of sessile plasmatocytes number in hematopoietic pockets that becomes
359 comparable to age-matched controls (grey bars) at later stages (day 11 and 13). Error bars
360 represent \pm SEM. (n = 5/genotype/age) P-value: *** $P < 0.001$; ** $P < 0.01$; * $P < 0.05$.

361 **3.4. Plasmatocytes display impaired phagocytic activity in HD condition.** We found that
362 the *Drosophila* model of HD displayed an altered hemocytes population. Even though mutant
363 HTT protein is expressed only in the neuronal population, peripheral immune cells appear
364 inflected at larval stage itself. To test whether the expression of mHTT under the control of
365 pan-neuronal elav-GAL4 driver could cause any detrimental effect on hemocyte functions,
366 we examined the phagocytic activity of plasmatocytes isolated from 3rd instar larvae and
367 adult at different ages post eclosion from control and diseased conditions. We quantified the
368 ability of plasmatocytes to engulf heat-killed propidium iodide (PI)-stained *E. coli* by
369 counting the number of cells capable of active phagocytosis. We found that plasmatocytes
370 isolated from diseased larvae showed a significant decline in percentage phagocytosis (n = 5;
371 $p = 0.006178$) compared to control condition (Fig. 4a & b). Moreover, diseased flies
372 exhibited a gradual decline in the phagocytic ability of plasmatocytes at indicated ages
373 compared to age-matched controls as disease progresses. In diseased adults, percentage
374 phagocytosis was comparable to normal at early age i.e. 1dpe that significantly reduced from
375 7dpe to 13dpe (n = 5; 7dpe, $p = 0.003398607$; day 11, $p = 3.92116E-06$; 13dpe, $p =$
376 0.000513315) (Fig. 4d). Instances can also be documented where a lesser number of bacteria
377 were phagocytized by a single plasmatocyte in diseased flies as compared to the age-matched
378 controls (Fig. 4c).

379 These results confirmed that impaired phagocytic activity of plasmatocytes in diseased
380 condition without targeting the expression of mHTT in immune cells is solely a consequence
381 of the diseased condition.

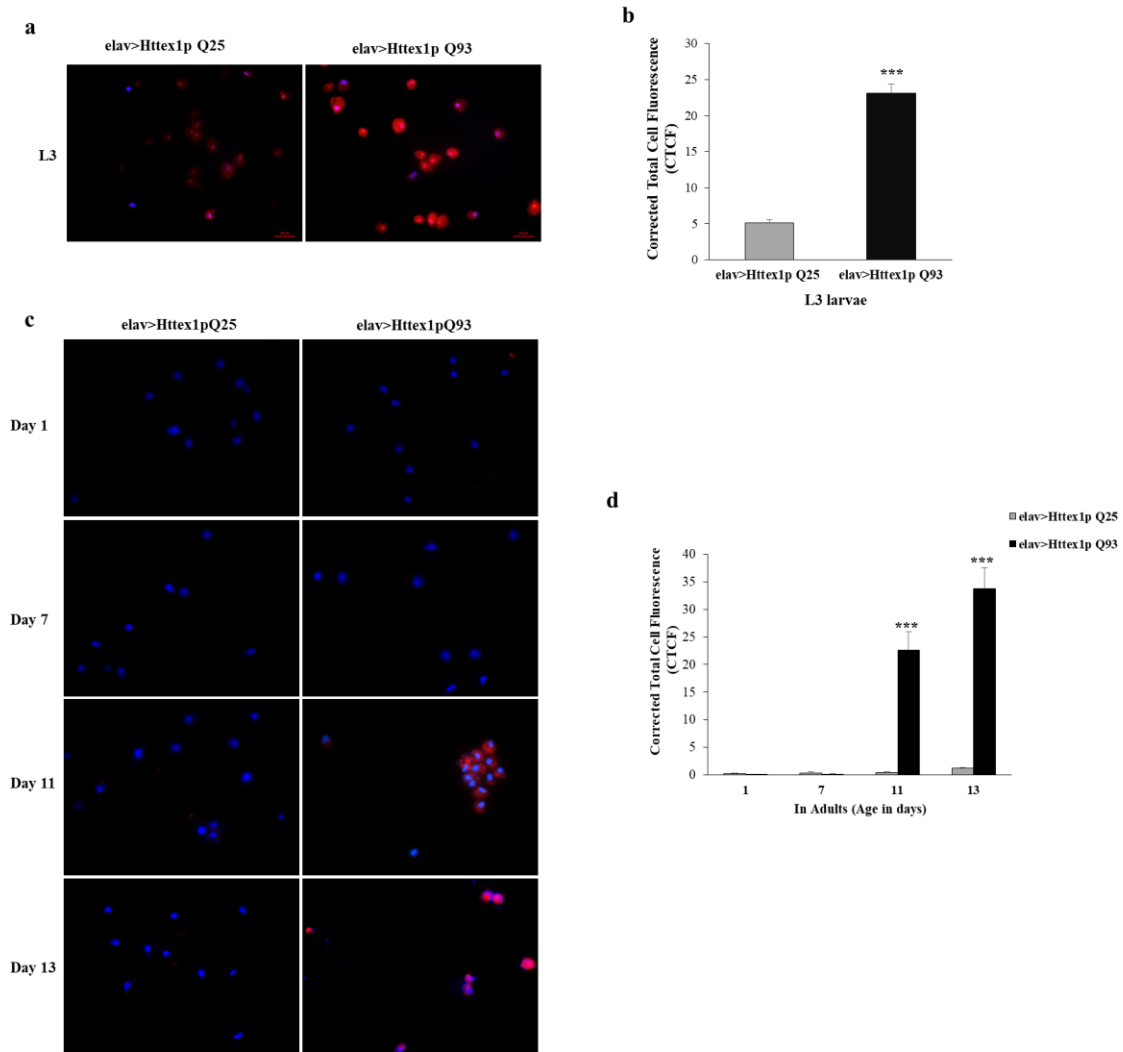


382

383 **Figure 4. Reduction in phagocytic activity of plasmatocytes in HD condition with**384 **disease progression. (a & c) Confocal microscope images showing the engulfment of heat-**385 **killed PI-stained *E. coli* DH5 α by plasmatocytes isolated from 25QHtt^{ex1} (control; left panel)**386 **and 93QHtt^{ex1} (diseased; right panel) expressing individuals at indicated ages. Scale bars**387 **represent 20 μ m. Phagocytic ability was calculated by counting the number of plasmatocytes**388 **showing phagocytosis per 100 plasmatocytes i.e., percentage phagocytosis. (b) Diseased**389 **larvae displayed a significant decline in phagocytic ability as compared to age-matched**

390 controls. (d) In diseased adults, the phagocytic ability of plasmatocytes was comparable to
391 control condition at initial stage i.e. day1. At later stages of disease (7dpe, 11dpe, and 13dpe),
392 the phagocytic ability of plasmatocytes was significantly reduced as compared to age-
393 matched controls. Error bars represent \pm SEM. (n = 5/genotype/age) P-value: *** $P < 0.001$;
394 ** $P < 0.01$; * $P < 0.05$.

395 **3.5. Enhanced ROS production in plasmatocytes of diseased larvae and flies at the**
396 **terminal stage of the disease.** Although HD may arise through several mechanisms,
397 oxidative stress, the result of altered cellular redox status, has emerged as a potential factor
398 involved in neurodegeneration and cell death in the etiology of HD. Phagocytes are the major
399 producers of reactive oxygen species during their activation and phagocytosis of microbes
400 and cellular debris. ROS are generally considered deleterious to cells, but ROS also has an
401 important role in regulating signal transduction pathways. There is a possibility that reactive
402 oxygen species generated by plasmatocytes could play a role in HD pathogenesis. Therefore,
403 to unravel possible mechanisms underlying the impaired phagocytosis activity of
404 plasmatocytes, we monitored levels of intracellular ROS in plasmatocytes in normal and
405 diseased conditions at the indicated ages with disease progression. We measured levels of
406 intracellular ROS in plasmatocytes of normal and diseased larvae. Cell permeable dye DHE
407 with high permeability and specificity for superoxide radicals generated upon oxidative stress
408 was used for ROS quantification. The intensity of DHE staining in cells/tissues is
409 proportionate to the ROS levels. Basal ROS levels were detected in the plasmatocytes of both
410 25Q^{Htt^{ex1}} and 93Q^{Htt^{ex1}} larvae. However, ROS signals in the plasmatocytes of diseased



411
 412 **Figure 5. Increased levels of ROS in plasmatocytes of HD condition.** (a & b) Estimation
 413 of ROS levels in circulating plasmatocytes isolated from 25QHtt^{ex1} (control; left panel) and
 414 93QHtt^{ex1} (diseased; right panel) expressing individuals at indicated ages.. Red =
 415 dihydroethidium (DHE) and, Blue = DAPI, scale bars represent 50µm. (c) Quantification of
 416 the images done using ImageJ software (n=5/genotype/age) revealed that plasmatocytes of
 417 93QHtt^{ex1} expressing larvae exhibit a significant increase in ROS intensity as compared to the
 418 age-matched controls and in adults (d) ROS levels remained comparable between diseased
 419 and control groups at 1dpe and 7dpe but were remarkably higher at 11dpe and 13dpe in the
 420 diseased group, as compared to the control group. Statistical analysis was done using

421 Student's t-test. * represents significance against age-matched control. Error bars represent \pm
422 SEM. P-value: *** $P < 0.001$; ** $P < 0.01$; * $P < 0.05$.

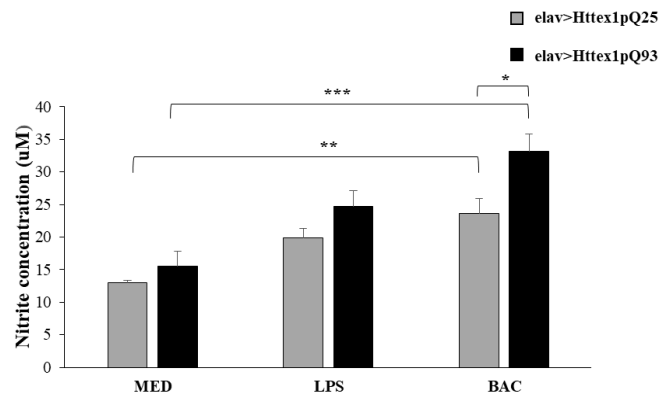
423 larvae were considerably higher as compared to age-matched controls (Fig. 5a). Further
424 quantification of DHE intensity as a representative of ROS levels confirmed that
425 plasmatocytes of diseased larvae exhibit significant elevation in ROS levels as compared to
426 age-matched controls (Fig. 5b). In adults, ROS level in diseased condition remains
427 comparable to the control condition during initial (1dpe) and symptomatic stages (7dpe),
428 whereas it increases significantly at later ages (11dpe; $p = 0.002733194$ and 13dpe; $p =$
429 0.000971124) (Fig. 5c & d). Further, diseased flies showed significantly high ROS at day13
430 in comparison to day11 counterparts which suggests that ROS levels increase with disease
431 progression. Taken together, we can establish that neuronal expression of mHTT results in
432 altered immune response, in the form of impaired phagocytosis, and increased ROS levels at
433 terminal age may be contributing to the surge in deaths observed.

434 **3.6. Increased nitrite production by plasmatocytes in HD larvae.**

435 Nitric oxide (NO) is involved in several physiological functions of the CNS, including
436 neurotransmission, memory, and synaptic plasticity. Excessive NO production, as elicited by
437 inflammatory signals, plays a key role in diverse neurodegenerative-associated processes such
438 as neuronal death, necrosis, apoptosis, and autophagy (Calabrese et al., 2007).

439 Thereby we further extended our study by evaluating the levels of nitrite production by
440 plasmatocytes *in vitro*. To monitor NO release by plasmatocytes we stimulated plasmatocytes
441 with LPS and bacterial challenge. We observed that basal levels (without stimulation) of
442 nitrite release by plasmatocytes isolated from diseased larvae is comparable to the control
443 condition. However, a significant increase in nitrite release by plasmatocytes of diseased
444 larvae is seen at 48 hours after LPS and bacterial treatment ($n = 3$, $p = 0.02915143$) as

445 compared to control condition (Fig. 6). As NO is principally involved in many immune
 446 signaling pathways, a higher concentration of NO in plasmatocytes of diseased condition may
 447 also be a reason for immune dysfunction.



448

449 **Figure 6. Increased nitrite production by *E. coli* treated plasmatocytes of diseased**
 450 **larvae.** The nitrite production was measured in the supernatant after 48 hours of LPS and
 451 bacterial challenge using the Griess reagent. Quantification of NO levels revealed a
 452 significant increase in NO production in diseased condition after 48 hrs of bacterial treatment.
 453 Statistical analysis was done using Student's t-test. Values are represented as \pm SEM;
 454 (n=3/genotype). P-value: *** $P < 0.001$; ** $P < 0.01$; * $P < 0.05$.

455 **4. Discussion**

456 The most predominant neuropathological feature in HD involves degeneration of a specific
 457 set of neurons in the striatum and cortical regions of brain that might give rise to
 458 characteristic clinical symptoms of the disease. In addition to neurobiological anomalies,
 459 immune dysregulation is considered one of the clinical challenges and may critically
 460 contribute to the pathology of HD. Previous studies from HD patients and mouse models
 461 have suggested that mHTT expression persuades both microglial activation in the HD brain
 462 and elevated levels of pro-inflammatory molecules released by peripheral immune cells such
 463 as monocytes and macrophages in the blood, supporting the idea that inflammation is not just

464 a repercussion of disease but an active contributor too (Björkqvist et al., 2008; Crotti et al.,
465 2014; Kwan et al., 2012). Since mHTT expresses ubiquitously in human patients and HD
466 mice, it is still unclear whether mutant protein contributes to immune dysregulation in the
467 cell-autonomous or non-cell-autonomous manner (Hoogeveen et al., 1993). In the present
468 study, we expressed the mHTT exon 1 fragment specifically in the neuronal cells of
469 *Drosophila* since the embryonic stage and assessed its detrimental non-cell-autonomous *in*
470 *vivo* effects on *Drosophila* hemocytes. Melanization reaction carried out by crystal cells of
471 *Drosophila* involves both humoral and cellular components of the innate immune system can
472 be used as a sensor of stress and environmental changes to elicit the necessary responses. A
473 phenotypic and quantitative examination of crystal cells demonstrated a significant increase
474 in crystal cell count in late 3rd instar larvae. Melanization has been considered an important
475 tool to minimize damage from physical and pathogenic stresses. Crystal cells possess
476 crystalline inclusions of prophenoloxidase (proPO) in their cytoplasm which gives them their
477 characteristic appearance. Under stressed conditions, the serine protease cascade may become
478 activated, ultimately cleaving proPO to their active form of phenoloxidase (PO). PO in turn
479 oxidizes phenols into quinones which subsequently polymerize to produce melanin (Meister
480 & Lagueux, 2003). Estimation of prophenoloxidase (PO) activity also showed that enzyme is
481 present in significantly high concentration in the hemolymph of diseased larvae. As crystal
482 cells are directly linked with the melanization process, their proliferation increases in
483 response to pathogenic stress to synthesize a more abundant amount of melanin to minimize
484 the damage caused by mutant protein. Moreover, activated PO results in the production of
485 reactive oxygen species during melanin biosynthesis that acts as a signaling molecule for
486 activation of other crucial immune responses
487 such as encapsulation, nodule formation, phagocytosis, and AMP production
488 (Cerenius et al., 2008). Likewise, a recent study demonstrated that during trauma, PO-

489 induced ROS activates JNK-dependent cytoprotective programs in neuronal tissue required
490 for systemic host protection (Nam et al., 2012).

491 We further investigated the number of circulating plasmatocytes in 3rd instar larvae of both
492 healthy and diseased conditions that exhibited a significant increase in circulating
493 plasmatocyte count in diseased condition. In line with these results, other studies have shown
494 the high plasmatocyte count in circulation in response to parasitoid infections is associated
495 with increased resistance against parasitoid wasps in several *Drosophila* species, although the
496 molecular mechanism behind this phenomenon is not inferred (Eslin and Prevost., 1998;
497 Kacsoh and Schlenke., 2012). Studies from several groups have extensively elucidated the
498 process of hematopoiesis in *Drosophila* during larval stage. *Drosophila* hematopoiesis at
499 larval stages occurs in two separate waves during development. The first wave of *Drosophila*
500 larval hematopoiesis is founded by differentiated hemocytes of the embryo, which colonize
501 segmentally repeated epidermal-muscular pockets and proliferate in these locations
502 (Makhijani et al., 2011; Makhijani and Bruckner, 2012). During larval hematopoiesis, sessile
503 plasmatocyte population undergoes a significant proliferation, expanding by self-renewal.⁴⁸
504 Moreover, during these developmental stages, plasmatocytes are characterized by a dynamic
505 behaviour, continuously exchanging between the sessile and circulating state. Like
506 plasmatocytes, crystal cells increase in number during larval stages. However, crystal cell
507 proliferation is not due to a self-renewal mechanism because mature crystal cells do not
508 divide. Instead, a recent study has shown that new crystal cells originate from trans-
509 differentiation of sessile plasmatocytes via a Notch–Serrate dependent process (Leitao and
510 Sucena., 2015). Second wave of hematopoiesis occurs late in larval development within the
511 lymph gland, a dedicated hematopoietic organ of mesoderm origin. Hematopoiesis in lymph
512 gland only occurs in response to stress or immune challenge by synchronous differentiation
513 of lymph gland prohemocytes (Krzemień et al., 2007; Grigorian et al., 2011; Gold and

514 Brückner, 2015; Banerjee et al., 2019). In our study, a high plasmacyte number of diseased
515 larvae might be an outcome of release of plasmacytes either from lymph gland or
516 hematopoietic pockets into the circulation. We further evaluated the propensity of neuronal-
517 specific expression of mHTT on plasmacytes of hematopoietic pockets in HD flies at
518 different ages and found an obstinate plasmacyte count in hematopoietic pockets/hubs of
519 diseased flies throughout disease progression whereas there was a gradual decline in
520 plasmacyte number in hematopoietic pockets of controls with aging. In the course of
521 metamorphosis, hemocytes from both the hematopoietic pockets or the lymph gland enter
522 into the circulation system and persist to adulthood as mixed population Lanot et al., 2001;
523 Gold and Brückner, 2015; Banerjee et al., 2019). Additionally, most studies claimed the lack
524 of new hemocyte production in adult *Drosophila*; that is consistent with increased
525 immunosenescence observed in aged adult flies Banerjee et al., 2019; Bosch et al., 2019;
526 Mackenzie et al., 2011), while one study claimed active hematopoietic activity in adult
527 *Drosophila* (Ghosh et al., 2015). Also, it has been reported that plasmacyte count in
528 hematopoietic hubs does not remain the same during adult life. There is a gradual increase in
529 the number after eclosion till 5 days post eclosion (dpe); thereafter remains relatively
530 constant up to 8 dpe and then declines as the age progress. This gradual loss of resident
531 plasmacytes suggests that adult employs plasmacytes from the hubs at it ages (Ghosh et
532 al., 2015). Additionally, it has been reported that sessile hematopoietic pockets are in close
533 contact with the peripheral nervous system (PNS) that provides an attractive and tropic
534 microenvironment for localization, survival, and proliferation to these resident hemocytes
535 (Makhijani et al., 2011). More recently, it has been shown that sensory neurons of the
536 peripheral nervous system produces Activin- β , which turned out to be an important factor in
537 the regulation of haemocyte proliferation and adhesion (Makhijani et al., 2017). Based on
538 these reports we assume that possibly mHTT expression in neurons is affecting production

539 and release of Activin- β or some unknown tropic factor from peripheral neurons which
540 subsequently maybe responsible for proliferation and release of plasmatocytes in circulation
541 as well as in trans-differentiation into crystal cells. However, further insight into the blood
542 cell differentiation and neuronal regulation of *Drosophila* hematopoietic sites, providing a
543 link between neuronal sensing and adaptive responses of local blood cell populations would
544 expand understanding of present work. In contradiction to our result, a previous study
545 showed that cell-autonomous expression of mHTT with hemocyte-specific driver causes a
546 significant reduction in the circulating plasmatocyte count in diseased larvae (Lin et al.,
547 2019). Our results ostensibly differ as we targeted mHTT expression specifically in neuronal
548 cells using pan-neuronal driver, *elav-Gal4* and assessed plasmatocyte number in a cell-non-
549 autonomous manner. However, similar to their results, we observed that despite a significant
550 increase in plasmatocyte count mHTT expression in neuronal cells results in decreased
551 phagocytic activity towards bacterial particles at both larval and later stages of disease
552 progression i.e., from 7dpe to 13 dpe. We found that a lesser number of plasmatocytes of
553 mHTT expressing flies were able to initiate phagocytosis and also passively engaged in
554 engulfment of bacterial particles compared to the healthy controls. Subsidiary our results,
555 studies from human patients also reported the compromised phagocytic activity of peripheral
556 monocytes in other neurodegenerative diseases such as AD and PD (Grozdánov et al., 2014;
557 Gu et al., 2016). In addition, defective actin remodeling in HD mouse immune cells leads to
558 failure of membrane ruffling, which supports our result since actin assembly is required to
559 trigger engulfment and phagolysosome maturation for successful phagocytosis (Kwan et al.,
560 2012; Swanson, 2008).

561 Further, we measured the levels of nitrite production by plasmatocytes because NO, a
562 fundamental signaling agent, participates in several physiological and pathological processes,
563 including immune response to microbes, neurodegenerative diseases, and asthma (Coleman,

2001; Nappi et al., 2000; Pacher et al., 2007). Increased nitrite release by LPS and bacterial stimulated plasmatocytes of mHTT expressing larvae indicates NO is a crucial factor that regulates immune sensitivity against challenges. NO, a volatile signaling agent, released from phagocytic cells may easily diffuse through BBB and further exacerbate cytotoxicity by NO mediating inflammatory response in *Drosophila* nervous tissues (Ellrichmann et al., 2013; Inamdar & Bennett, 2013; Parathath et al., 2006). Indeed, previous studies have shown that induced NO release from the hemocytes leads to the activation of antimicrobial peptides in the fat body (Foley and O'Farrell., 2003). To gain a mechanistic understanding of dysregulated peripheral immune response in diseased condition, we investigated the status of reactive oxygen species (ROS) in plasmatocytes of mHTT expressing larvae and flies with disease progression. Consistent with previous studies in HD patients, we observed significantly high ROS levels in circulating plasmatocytes of 3rd instar larvae and resident plasmatocytes at advanced disease stages i.e. 11dpe and 13 dpe as compared to age-matched controls which might be the outcome of aggravated inflammatory environment and metabolic dysregulation in immune cells. Earlier Chen et al. and Hersch et al. reported increased oxidative damage and suppressed anti-oxidant capacity of peripheral immune cells in HD patients (Chen et al., 2007; Hersch et al., 2006). It is well documented that ROS is critical to macrophage phagocytic activity. Notably, diseases associated with chronic inflammation display impaired macrophage phagocytic activity that is correlated with changes in the ROS signalling (Forrester et al., 2018). The available evidence, however, indicates that non-cell-autonomous expression of mHTT dysregulates peripheral immune response, although the underlying mechanisms are yet to be elucidated.

To our knowledge, this is the first *in vivo* report showing that expression of mHTT exon1 fragment exclusively in neuronal cells is sufficient to cause immune dysregulation in *Drosophila* hemocytes in a non-cell-autonomous manner. It might also possible that the

589 recognition and clearance of mutant protein aggregates by microglia and astrocytes in the
590 brain triggers innate immune response including the release of pro-inflammatory cytokines,
591 which subsequently distress circulating immune cells (Heneka et al., 2014; Tian et al., 2012).
592 The dysregulated immune response of peripheral immune cells may be, at least in part,
593 responsible for the toxicity of mutant Huntingtin proteins on peripheral tissues and the
594 progression of HD. Further insights into the molecular mechanism of phagocytosis
595 suppression and molecular interactions between mHTT and immune signaling pathways
596 would facilitate the quest for novel therapeutic interventions aimed to alleviate HD pathology
597 and improving the quality of life of the patients.

598 **Acknowledgment**

599 This work was financially supported by the University of Delhi. J.D. acknowledges the
600 University Grant Commission (UGC), India for financial aid received in the form of research
601 fellowship. We would like to thank Prof. J. Lawrence Marsh, University of California, Irvine,
602 CA, USA for generously gifting polyQ lines and GAL4 driver lines.

603 **Disclosure of Ethical Statements**

604 **Approval of research protocol:** No human participant was involved in this study.

605 **Informed Consent:** N/A

606 **Registry and the Registration No. of the study/trial:** N/A

607 **Animal studies:** All animal experiments were conducted following the national and
608 international guidelines and the relevant national laws on the protection of animals. All
609 experiments of this study were conducted using *Drosophila* and it remains out of bioethical
610 considerations.

611 **Funding**

612 This research did not receive any specific grant from funding agencies in the public,
613 commercial, or not-for-profit sectors.

614 **Author's contributions**

615 J.D., N.A., and A.S. conceptualized, designed, and analyzed the experiments. J.D. performed
616 the experiments and wrote the original draft. N.A. and A.S. reviewed and edited the
617 manuscript. All authors read the manuscript carefully.

618 **Conflict of Interest**

619 The authors declare no conflict of interest.

620 **References**

621 Andre, R., Carty, L. and Tabrizi, S.J., 2016. Disruption of immune cell function by mutant
622 huntingtin in Huntington's disease pathogenesis. *Current opinion in pharmacology*, 26,
623 pp.33-38.

624 Andrew, S.E., Goldberg, Y.P., Kremer, B., Telenius, H., Theilmann, J., Adam, S., Starr, E.,
625 Squitieri, F., Lin, B., Kalchman, M.A. and Graham, R.K., 1993. The relationship between
626 trinucleotide (CAG) repeat length and clinical features of Huntington's disease. *Nature*
627 *genetics*, 4(4), pp.398-403.

628 Banerjee, U., Girard, J.R., Goins, L.M. and Spratford, C.M., 2019. Drosophila as a genetic
629 model for hematopoiesis. *Genetics*, 211(2), pp.367-417.

630 Bates, G., Harper, P. and Jones, L., 2002. Huntington's disease. Oxford University Press,
631 USA

632 Bjorkqvist, M., Wild, E.J., Thiele, J., Silvestroni, A., Andre, R., Lahiri, N., Raibon, E., Lee,
633 R.V., Benn, C.L., Soulet, D. and Magnusson, A., 2008. A novel pathogenic pathway of
634 immune activation detectable before clinical onset in Huntington's disease. *The Journal of*
635 *experimental medicine*, 205(8), pp.1869-1877.

636 Bosch, P.S., Makhijani, K., Herboso, L., Gold, K.S., Baginsky, R., Woodcock, K.J.,
637 Alexander, B., Kukar, K., Corcoran, S., Jacobs, T. and Ouyang, D., 2019. Adult *Drosophila*
638 lack hematopoiesis but rely on a blood cell reservoir at the respiratory epithelia to relay
639 infection signals to surrounding tissues. *Developmental Cell*, 51(6), pp.787-803.

640 Bouchard, J., Truong, J., Bouchard, K., Dunkelberger, D., Desrayaud, S., Moussaoui, S.,
641 Tabrizi, S.J., Stella, N. and Muchowski, P.J., 2012. Cannabinoid receptor 2 signaling in
642 peripheral immune cells modulates disease onset and severity in mouse models of
643 Huntington's disease. *Journal of Neuroscience*, 32(50), pp.18259-18268.

644 Bradford, J., Shin, J.Y., Roberts, M., Wang, C.E., Li, X.J. and Li, S., 2009. Expression of
645 mutant huntingtin in mouse brain astrocytes causes age-dependent neurological
646 symptoms. *Proceedings of the National Academy of Sciences*, 106(52), pp.22480-22485.

647 Bradford, M.M., 1976. A rapid and sensitive method for the quantitation of microgram
648 quantities of protein utilizing the principle of protein-dye binding. *Analytical*
649 *biochemistry*, 72(1-2), pp.248-254.

650 Brand, A.H. and Perrimon, N., 1993. Targeted gene expression as a means of altering cell
651 fates and generating dominant phenotypes. *development*, 118(2), pp.401-415.

652 Calabrese, V., Mancuso, C., Calvani, M., Rizzarelli, E., Butterfield, D.A. and Stella, A.M.G.,
653 2007. Nitric oxide in the central nervous system: neuroprotection versus
654 neurotoxicity. *Nature Reviews Neuroscience*, 8(10), pp.766-775.

655 Cerenius, L., Lee, B.L. and Söderhäll, K., 2008. The proPO-system: pros and cons for its role
656 in invertebrate immunity. *Trends in immunology*, 29(6), pp.263-271.

657 Chen, C.M., Wu, Y.R., Cheng, M.L., Liu, J.L., Lee, Y.M., Lee, P.W., Soong, B.W. and Chiu,
658 D.T.Y., 2007. Increased oxidative damage and mitochondrial abnormalities in the peripheral
659 blood of Huntington's disease patients. *Biochemical and biophysical research*
660 *communications*, 359(2), pp.335-340.

- 661 Coleman, J.W., 2001. Nitric oxide in immunity and inflammation. *International*
662 *immunopharmacology*, 1(8), pp.1397-1406.
- 663 Crotti, A., Benner, C., Kerman, B.E., Gosselin, D., Lagier-Tourenne, C., Zuccato, C.,
664 Cattaneo, E., Gage, F.H., Cleveland, D.W. and Glass, C.K., 2014. Mutant Huntingtin
665 promotes autonomous microglia activation via myeloid lineage-determining factors. *Nature*
666 *neuroscience*, 17(4), pp.513-521.
- 667 Dhankhar, J., Agrawal, N. and Shrivastava, A., 2020. An interplay between immune response
668 and neurodegenerative disease progression: an assessment using *Drosophila* as a
669 model. *Journal of Neuroimmunology*, 346, p.577302.
- 670 Ding, A.H., Nathan, C.F. and Stuehr, D.J., 1988. Release of reactive nitrogen intermediates
671 and reactive oxygen intermediates from mouse peritoneal macrophages. Comparison of
672 activating cytokines and evidence for independent production. *The Journal of*
673 *Immunology*, 141(7), pp.2407-2412.
- 674 Donley, D.W., Olson, A.R., Raisbeck, M.F., Fox, J.H. and Gigley, J.P., 2016. Huntingtons
675 disease mice infected with *Toxoplasma gondii* demonstrate early kynurenine pathway
676 activation, altered CD8+ T-cell responses, and premature mortality. *PLoS One*, 11(9),
677 p.e0162404.
- 678 Ellrichmann, G., Reick, C., Saft, C. and Linker, R.A., 2013. The role of the immune system
679 in Huntington's disease. *Clinical and Developmental Immunology*, 2013.
- 680 Elrod-Erickson, M., Mishra, S. and Schneider, D., 2000. Interactions between the cellular and
681 humoral immune responses in *Drosophila*. *Current Biology*, 10(13), pp.781-784.
- 682 Eslin, P. and Prévost, G., 1998. Hemocyte load and immune resistance to *Asobara tabida* are
683 correlated in species of the *Drosophila melanogaster* subgroup. *Journal of Insect*
684 *Physiology*, 44(9), pp.807-816.

685 Foley, E. and O'Farrell, P.H., 2003. Nitric oxide contributes to induction of innate immune
686 responses to gram-negative bacteria in *Drosophila*. *Genes & development*, *17*(1), pp.115-125.

687 Forrester, S.J., Kikuchi, D.S., Hernandez, M.S., Xu, Q. and Griendling, K.K., 2018. Reactive
688 oxygen species in metabolic and inflammatory signaling. *Circulation research*, *122*(6),
689 pp.877-902.

690 Ghosh, S., Singh, A., Mandal, S. and Mandal, L., 2015. Active hematopoietic hubs in
691 *Drosophila* adults generate hemocytes and contribute to immune response. *Developmental*
692 *cell*, *33*(4), pp.478-488.

693 Gold, K.S. and Brückner, K., 2015, December. Macrophages and cellular immunity in
694 *Drosophila melanogaster*. In *Seminars in Immunology* (Vol. 27, No. 6, pp. 357-368).
695 Academic Press.

696 Grigorian, M., Mandal, L. and Hartenstein, V., 2011. Hematopoiesis at the onset of
697 metamorphosis: terminal differentiation and dissociation of the *Drosophila* lymph
698 gland. *Development genes and evolution*, *221*(3), pp.121-131.

699 Grozdanov, V., Bliederaeuser, C., Ruf, W.P., Roth, V., Fundel-Clemens, K., Zondler, L.,
700 Brenner, D., Martin-Villalba, A., Hengerer, B., Kassubek, J. and Ludolph, A.C., 2014.
701 Inflammatory dysregulation of blood monocytes in Parkinson's disease patients. *Acta*
702 *neuropathologica*, *128*(5), pp.651-663.

703 Gu, B.J., Huang, X., Ou, A., Rembach, A., Fowler, C., Avula, P.K., Horton, A., Doecke, J.D.,
704 Villemagne, V.L., Macaulay, S.L. and Maruff, P., 2016. Innate phagocytosis by peripheral
705 blood monocytes is altered in Alzheimer's disease. *Acta neuropathologica*, *132*(3), pp.377-
706 389.

707 Hanisch, U.K., 2002. Microglia as a source and target of cytokines. *Glia*, *40*(2), pp.140-155.

708 Heneka, M.T., Kummer, M.P. and Latz, E., 2014. Innate immune activation in
709 neurodegenerative disease. *Nature Reviews Immunology*, *14*(7), pp.463-477.

710 Hersch, S.M., Gevorkian, S., Marder, K., Moskowitz, C., Feigin, A., Cox, M., Como, P.,
711 Zimmerman, C., Lin, M., Zhang, L. and Ulug, A.M., 2006. Creatine in Huntington disease is
712 safe, tolerable, bioavailable in brain and reduces serum 8OH^{2'} dG. *Neurology*, 66(2), pp.250-
713 252.

714 Ho, L.W., Carmichael, J., Swartz, J., Wytttenbach, A., Rankin, J. and Rubinsztein, D.C.,
715 2001. The molecular biology of Huntington's disease. *Psychological medicine*, 31(1), pp.3-
716 14.

717 Hoogeveen, A.T., Willemsen, R., Meyer, N., Roolj, K.E.D., Roos, R.A., Ommen, G.J.B.V.
718 and Galjaard, H., 1993. Characterization and localization of the Huntington disease gene
719 product. *Human molecular genetics*, 2(12), pp.2069-2073.

720 Inamdar, A. and Bennett, J., 2013. Fungal volatile organic compounds: Biogenic toxins as
721 etiological agents for Parkinson's disease. *Journal of the Neurological Sciences*, 333, p.e80.

722 Jennings, B.H., 2011. Drosophila—a versatile model in biology & medicine. *Materials*
723 *today*, 14(5), pp.190-195.

724 Kacsoh, B.Z. and Schlenke, T.A., 2012. High hemocyte load is associated with increased
725 resistance against parasitoids in *Drosophila suzukii*, a relative of *D. melanogaster*. *PLoS*
726 *one*, 7(4), p.e34721.

727 Kim, S.U. and de Vellis, J., 2005. Microglia in health and disease. *Journal of neuroscience*
728 *research*, 81(3), pp.302-313.

729 Kotrcova, E., Jarkovska, K., Valekova, I., Zizkova, M., Motlik, J., Gadher, S.J. and
730 Kovarova, H., 2015. Challenges of Huntington's disease and quest for therapeutic
731 biomarkers. *PROTEOMICS—Clinical Applications*, 9(1-2), pp.147-158.

732 Krzemiń, J., Dubois, L., Makki, R., Meister, M., Vincent, A. and Crozatier, M., 2007.
733 Control of blood cell homeostasis in *Drosophila* larvae by the posterior signalling
734 centre. *Nature*, 446(7133), pp.325-328.

735 Kwan, W., Träger, U., Davalos, D., Chou, A., Bouchard, J., Andre, R., Miller, A., Weiss, A.,
736 Giorgini, F., Cheah, C. and Möller, T., 2012. Mutant huntingtin impairs immune cell
737 migration in Huntington disease. *The Journal of clinical investigation*, 122(12), pp.4737-
738 4747.

739 Lanot, R., Zachary, D., Holder, F. and Meister, M., 2001. Postembryonic hematopoiesis in
740 *Drosophila*. *Developmental biology*, 230(2), pp.243-257.

741 Leblhuber, F., Walli, J., Jellinger, K., Tilz, G.P., Widner, B., Laccone, F. and Fuchs, D.,
742 1998. Activated immune system in patients with Huntington's disease.

743 Leitao, A.B. and Sucena, E., 2015. *Drosophila* sessile hemocyte clusters are true
744 hematopoietic tissues that regulate larval blood cell differentiation. *Elife*, 4, p.e06166.

745 Lemaitre, B. and Hoffmann, J., 2007. The host defense of *Drosophila melanogaster*. *Annu.*
746 *Rev. Immunol.*, 25, pp.697-743.

747 Lin, Y.H., Maaroufi, H.O., Ibrahim, E., Kucerova, L. and Zurovec, M., 2019. Expression of
748 human mutant huntingtin protein in *Drosophila* hemocytes impairs immune
749 responses. *Frontiers in immunology*, 10, p.2405.

750 MacDonald, M.E., Ambrose, C.M., Duyao, M.P., Myers, R.H., Lin, C., Srinidhi, L., Barnes,
751 G., Taylor, S.A., James, M., Groot, N. and MacFarlane, H., 1993. A novel gene containing a
752 trinucleotide repeat that is expanded and unstable on Huntington's disease
753 chromosomes. *Cell*, 72(6), pp.971-983.

754 Mackenzie, D.K., Bussi re, L.F. and Tinsley, M.C., 2011. Senescence of the cellular immune
755 response in *Drosophila melanogaster*. *Experimental gerontology*, 46(11), pp.853-859.

756 Makhijani, K. and Br ckner, K., 2012. Of blood cells and the nervous system: hematopoiesis
757 in the *Drosophila* larva. *Fly*, 6(4), pp.254-260.

758 Makhijani, K., Alexander, B., Rao, D., Petraki, S., Herboso, L., Kukar, K., Batool, I.,
759 Wachner, S., Gold, K.S., Wong, C. and O'Connor, M.B., 2017. Regulation of *Drosophila*

- 760 hematopoietic sites by Activin- β from active sensory neurons. *Nature communications*, 8(1),
761 pp.1-12.
- 762 Makhijani, K., Alexander, B., Tanaka, T., Rulifson, E. and Brückner, K., 2011. The
763 peripheral nervous system supports blood cell homing and survival in the *Drosophila*
764 larva. *Development*, 138(24), pp.5379-5391.
- 765 Marques Sousa, C. and Humbert, S., 2013. Huntingtin: here, there, everywhere!. *Journal of*
766 *Huntington's disease*, 2(4), pp.395-403.
- 767 Marsh, J.L., Walker, H., Theisen, H., Zhu, Y.Z., Fielder, T., Purcell, J. and Thompson, L.M.,
768 2000. Expanded polyglutamine peptides alone are intrinsically cytotoxic and cause
769 neurodegeneration in *Drosophila*. *Human molecular genetics*, 9(1), pp.13-25.
- 770 Meister, M. and Lagueux, M., 2003. *Drosophila* blood cells. *Cellular microbiology*, 5(9),
771 pp.573-580.
- 772 Moffitt, H., McPhail, G.D., Woodman, B., Hobbs, C. and Bates, G.P., 2009. Formation of
773 Polyglutamine Inclusions in a Wide Range of Non-CNS Tissues in the Hdh Q150 Knock-In
774 Mouse Model of Huntington's Disease. *PloS one*, 4(11), p.e8025.
- 775 Nam, H.J., Jang, I.H., You, H., Lee, K.A. and Lee, W.J., 2012. Genetic evidence of a redox-
776 dependent systemic wound response via Hyan protease-phenoloxidase system in
777 *Drosophila*. *The EMBO journal*, 31(5), pp.1253-1265.
- 778 Nappi, A.J., Vass, E., Frey, F. and Carton, Y., 2000. Nitric oxide involvement in *Drosophila*
779 immunity. *Nitric oxide*, 4(4), pp.423-430.
- 780 Neyen, C., Bretscher, A.J., Binggeli, O. and Lemaitre, B., 2014. Methods to study *Drosophila*
781 immunity. *Methods*, 68(1), pp.116-128.
- 782 Pacher, P., Beckman, J.S. and Liaudet, L., 2007. Nitric oxide and peroxynitrite in health and
783 disease. *Physiological reviews*, 87(1), pp.315-424.

784 Palazuelos, J., Davoust, N., Julien, B., Hatterer, E., Aguado, T., Mechoulam, R., Benito, C.,
785 Romero, J., Silva, A., Guzmán, M. and Nataf, S., 2008. The CB2 cannabinoid receptor
786 controls myeloid progenitor trafficking: involvement in the pathogenesis of an animal model
787 of multiple sclerosis. *Journal of Biological Chemistry*, 283(19), pp.13320-13329.

788 Parathath, S.R., Parathath, S. and Tsirka, S.E., 2006. Nitric oxide mediates neurodegeneration
789 and breakdown of the blood-brain barrier in tPA-dependent excitotoxic injury in
790 mice. *Journal of cell science*, 119(2), pp.339-349.

791 Rizki, T.M., Rizki, R.M. and Grell, E.H., 1980. A mutant affecting the crystal cells in
792 *Drosophila melanogaster*. *Wilhelm Roux's archives of developmental biology*, 188(2), pp.91-
793 99.

794 Sassone, J., Colciago, C., Cislighi, G., Silani, V. and Ciammola, A., 2009. Huntington's
795 disease: the current state of research with peripheral tissues. *Experimental neurology*, 219(2),
796 pp.385-397.

797 Sathasivam, K., Hobbs, C., Mangiarini, L., Mahal, A., Turmaine, M., Doherty, P., Davies,
798 S.W. and Bates, G.P., 1999. Transgenic models of Huntington's disease. *Philosophical*
799 *Transactions of the Royal Society of London. Series B: Biological Sciences*, 354(1386),
800 pp.963-969.

801 Steffan, J.S., Bodai, L., Pallos, J., Poelman, M., McCampbell, A., Apostol, B.L., Kazantsev,
802 A., Schmidt, E., Zhu, Y.Z., Greenwald, M. and Kurokawa, R., 2001. Histone deacetylase
803 inhibitors arrest polyglutamine-dependent neurodegeneration in
804 *Drosophila*. *Nature*, 413(6857), pp.739-743.

805 Streit, W.J., 2002. Microglia as neuroprotective, immunocompetent cells of the
806 CNS. *Glia*, 40(2), pp.133-139.

807 Swanson, J.A., 2008. Shaping cups into phagosomes and macropinosomes. *Nature reviews*
808 *Molecular cell biology*, 9(8), pp.639-649.

- 809 Tai, Y.F., Pavese, N., Gerhard, A., Tabrizi, S.J., Barker, R.A., Brooks, D.J. and Piccini, P.,
810 2007. Imaging microglial activation in Huntington's disease. *Brain research bulletin*, 72(2-3),
811 pp.148-151.
- 812 Taylor, J.P., Taye, A.A., Campbell, C., Kazemi-Esfarjani, P., Fischbeck, K.H. and Min, K.T.,
813 2003. Aberrant histone acetylation, altered transcription, and retinal degeneration in a
814 *Drosophila* model of polyglutamine disease are rescued by CREB-binding protein. *Genes &*
815 *development*, 17(12), pp.1463-1468.
- 816 Tian, L., Ma, L., Kaarela, T. and Li, Z., 2012. Neuroimmune crosstalk in the central nervous
817 system and its significance for neurological diseases. *Journal of neuroinflammation*, 9(1),
818 pp.1-10.
- 819 Valadão, P.A.C., da Silva Oliveira, B., Joviano-Santos, J.V., Vieira, É.L.M., Rocha, N.P.,
820 Teixeira, A.L., Guatimosim, C. and de Miranda, A.S., 2019. Inflammatory changes in
821 peripheral organs in the BACHD murine model of Huntington's disease. *Life sciences*, 232,
822 p.116653.
- 823 Wang, Q., Rowan, M.J. and Anwyl, R., 2004. β -amyloid-mediated inhibition of NMDA
824 receptor-dependent long-term potentiation induction involves activation of microglia and
825 stimulation of inducible nitric oxide synthase and superoxide. *Journal of*
826 *Neuroscience*, 24(27), pp.6049-6056.
- 827 Zehring, W.A., Wheeler, D.A., Reddy, P., Konopka, R.J., Kyriacou, C.P., Rosbash, M. and
828 Hall, J.C., 1984. P-element transformation with period locus DNA restores rhythmicity to
829 mutant, arrhythmic *Drosophila melanogaster*. *Cell*, 39(2), pp.369-376.